Carbon, J., & Squires, C. (1971) *Cancer Res. 31*, 663–666.
Donis-Keller, H., Maxam, A. M., & Gilbert, W. (1977) *Nucleic Acids Res. 4*, 2527–2538.
England, T. E., Bruce, A. G., & Uhlenbeck, O. C. (1980) *Methods Enzymol. 65*, 65–74.
Faulhammer, G., & Cramer, F. (1977) *Biochemistry 16*, 561–570.
Johnson, P. F., & Abelson, J. (1983) *Nature (London) 302*, 681–687.
Johnson, R. A., & Walseth, T. F. (1979) *Adv. Cyclic Nucleotide Res. 10*, 35–167.
Kisselev, L. L. (1983) *Mol. Biol. 17*, 928–948.
Kisselev, L. L., & Frolova, L. Yu (1964) *Biokhimiya (Moscow) 29*, 1177–1189.
Klee, C. B. (1971) *Proced. Nucleic Acid Res. 2*, 896.
Lestienne, P. (1978) *J. Theor. Biol. 73*, 159–180.
Loftfield, R. B., Eigner, E. A., & Pastuszyn, A. (1981) *J. Biol. Chem. 256*, 6729–6735.
Maxwell, H. I., Wimmer, E., & Tener, G. M. (1968) *Biochemistry 7*, 2629–2634.
McCutchan, T., Silverman, S., Kohli, J., & Söll, D. (1978) *Biochemistry 17*, 1662–1628.
McFarland, G., & Borer, P. (1979) *Nucleic Acids Res. 7*, 1067–1080.
Mohr, S., & Thach, R. (1969) *J. Biol. Chem. 244*, 6566–6576.
Moseman-McCoy, M. I., Lubben, T. H., & Gumport, R. I. (1979) *Biochim. Biophys. Acta 562*, 149.
Naylor, R., & Gilham, P. T. (1966) *Biochemistry 5*, 2722–2728.
Nishimura, S. (1979) in *Transfer RNA: Structure*, Properties, & Recognition (Schimmel, P. R., Söll, D., & Abelson, J. N., Eds.) pp 551–552, Cold Spring Harbor Laboratory, Cold Spring Harbor, NY.
Roe, B., Michael, M., & Dudock, B. (1973a) *Nature (London), New Biol. 246*, 135–137.
Roe, B., Sirover, M., & Dudock, B. (1973b) *Biochemistry 12*, 4146–4154.
Schulman, L. H., & Pelka, H. (1977) *Biochemistry 16*, 4256–4265.
Schulman, L. H., & Pelka, H. (1983a) *Nucleic Acids Res. 11*, 1439–1446.
Schulman, L. H., & Pelka, H. (1983b) *Proc. Natl. Acad. Sci. U.S.A. 80*, 6755–6759.
Soltis, D., & Uhlenbeck, O. C. (1982) *J. Biol. Chem. 257*, 11332–11339.
Thach, R. E., & Doty, P. (1965) *Science (Washington, D.C.) 147*, 1310–1311.
von der Haar, F., & Cramer, F. (1976) *Biochemistry 15*, 4131–4138.
Yarus, M., Knowlton, R., & Söll, L. (1977) in *Nucleic Acid-Protein Recognition*, pp 391–408, Academic Press, New York.

Phosphorylation and Methylation of *Physarum* Histone H1 during Mitotic Cycle†

Andrzej Jerzmanowski* and Marek Maleszewski‡
Department of Biochemistry, Warsaw University, 02-089 Warsaw, Żwirki i Wigury 93, Poland
Received July 5, 1984

ABSTRACT: We have shown that the heterogeneity of the typical histone H1 from the lower eukaryote *Physarum polycephalum* seen in sodium dodecyl sulfate ($NaDodSO_4$) gel electrophoresis is due principally to conformational effects produced by postsynthetic modifications rather than primary sequence variants. We have also shown by labeling with L-[*methyl*-^{3}H]methionine and amino acid analysis that *Physarum* H1 in addition to already known phosphorylation undergoes methylation on ϵ-NH_2 groups of several of its lysines. The analysis of *Physarum* H1 phosphorylation by high-resolution acetic acid–urea gel electrophoresis revealed that it could accept up to more than 20 phosphates per molecule. The mitotic cycle analysis of postsynthetic modifications of *Physarum* H1 showed that (a) H1 undergoes superphosphorylation in mitosis accepting from about 14 to more than 20 phosphates per molecule and (b) it is not totally dephosphorylated in the following cycle retaining from about 8 to about 16 phosphates per molecule in G2 phase. The results of this work are consistent with the interpretation that the newly synthesized H1 is deposited on DNA in nonmethylated and nonphosphorylated forms and its methylation (which is irreversible) precedes its phosphorylation in the course of chromatin maturation. The studies of *Physarum* H1 bisected with chymotrypsin indicate that most of the phosphorylation sites including the superphosphorylation in mitosis are localized in a larger COOH-terminal part of the molecule. The analysis of highly phosphorylated *Physarum* H1 by high-resolution $NaDodSO_4$ gel electrophoresis showed the existence of several discrete conformational subspecies resembling in their electrophoretic appearance the true sequence variants of mammalian H1.

Histone H1 plays a key role in the structural transitions of the basic 100-Å nucleosomal filament into the thick chromatin fiber, the 300-Å solenoid (Thoma et al., 1979). On the other hand, H1 shows a considerable degree of variability. Both the sequence variants of H1 and the postsynthetically modified H1 molecules usually occur at the same time in the same chromatin (Hohmann, 1983; Cole, 1984). This together has led to the suggestion that H1 through its different sequence variants and chemically modified subspecies (mostly by phosphorylation) may specifically influence the local conformation of chromatin and through it the genetic activity

† This work was supported by Polish Academy of Sciences Project 09.7 and by the Alexander von Humboldt Stiftung, Federal Republic of Germany.
‡ M.M. was a graduate student at the Department of Biochemistry, Warsaw University (1983–1984). Present address: Department of Embryology, Warsaw University, 00-035 Warsaw, Krakowskie Przedmieście 26/28, Poland.

0006-2960/85/0424-2360$01.50/0

(Hohmann, 1983). On the other hand, the occurrence of unspecific, mitotic superphosphorylation of H1 has been implicated in the process of mitotic condensation of chromosomes (Bradbury et al., 1974).

Most studies on the H1 sequence variants and phosphorylation in proliferating cells have been done on synchronous mammalian cell cultures. Both in Chinese hamster CHO cells and in HeLa cells the H1 histone subtypes undergo specific phosphorylations and dephosphorylations throughout the cell cycle. In these systems the cyclic superphosphorylation occurring in mitosis results in the introduction of four to six phosphate groups per molecule of H1 (Gurley et al., 1978; Ajiro et al., 1981).

The lower eukaryote *Physarum polycephalum* is particularly suited for cell cycle studies due to the perfect and completely natural synchrony of nuclear divisions (Mohberg, 1975). The pattern of phosphorylation of histone H1 has been studied in this organism by Bradbury et al. (1974) and by Fischer & Laemmli (1980). Whereas Bradbury et al. found the pattern of phosphorylation similar to that of CHO cells, Fischer & Laemmli, while confirming the premitotic increase in the phosphate content of H1, did not find a decrease in that phosphorylation after mitosis.

In this paper we give a detailed analysis of *Physarum* histone H1 and demonstrate that during the mitotic cycle in addition to extensive phosphorylation it undergoes methylation on ϵ-NH_2 groups of several of its lysines. We also reexamine the H1 phosphorylation pattern estimating the number of phosphates in H1 at different points of the mitotic cycle and demonstrate the existence of cyclic, mitotic superphosphorylation. We also analyze the preference of the phosphorylation and methylation in respect to NH_2- and COOH-terminal regions of the H1 molecule as well as the relationship between methylation and phosphorylation in the mitotic cycle.

Materials and Methods

Physarum Culture. Microplasmodia of the M3C strain of *P. polycephalum* were grown in shaken culture in semidefined medium as described previously (Daniel & Baldwin, 1964). Synchronous macroplasmodia were prepared according to Mittermayer et al. (1965). The position in the mitotic cycle was determined by examining the nuclear morphology by phase-contrast microscopy. The first synchronous mitosis occurred after 6–7 h and the second, third, and fourth occurred in 8.5–10.5-h intervals thereafter. The experiments were usually performed on macroplasmodia between second and third and third and fourth mitosis. In the latter case, filter papers with growing macroplasmodia were transfered on fresh media after mitosis III. Before processing, the initial inocula were removed from macroplasmodia.

Labeling. For labeling with $^{32}PO_4$, microplasmodia were washed several times with the semidefined medium from which the KH_2PO_4 has been omitted and inoculated in the same medium containing 60 μCi/mL $^{32}PO_4$ (Amersham "carrier free", in H_2O). The culture was grown for a further 48 h, and the material was collected. For labeling with L-[*methyl*-^{3}H]methionine (Amersham, in H_2O), microplasmodia from a 24-h culture were washed several times with the semidefined medium from which the protein hydrolysates had been omitted and transfered to the same medium containing 5 μCi/mL L-[*methyl*-^{3}H]methionine with or without cycloheximide (10 μg/mL). The culture was allowed to grow for a further 8 h, and the material was collected.

Isolation of Nuclei and Chromatin. Nuclei and chromatin were isolated from microplasmodia essentially as described by Jockusch & Walker (1974) except that 0.05% instead of 0.1% Triton X-100 was used in the homogenization and dense sucrose solutions. All solutions including the initial washing solution contained 1 mM PMSF (phenylmethanesulfonyl fluoride) and 1 mM PCMB (4-(hydroxymercuri)benzoic acid) to inhibit proteolytic and phosphatase activity, respectively. For the large-scale isolation of histone H1, nuclei were obtained by a simpler procedure in which the centrifugation through the dense sucrose solution had been omitted.

Isolation of Physarum Histone H1. Histone H1 was isolated from microplasmodial nuclei and chromatin and from whole synchronous macroplasmodia by the guanidine hydrochloride procedure described by Mende et al. (1983). H1 was finally separated from the rest of histones by selective extraction with 5% perchloric acid. The preparation obtained by the above procedure usually contained less than 20% contaminations and was used in all experiments except amino acid analysis.

Purification of Physarum Histone H1 by Electroelution. The preparation of *Physarum* histone H1 was further purified by preparative electrophoresis in sodium dodecyl sulfate ($NaDodSO_4$)–polyacrylamide gel containing the linear gradient of methylenebis(acrylamide) (see Polyacrylamide Gel Electrophoresis for detailes). A total of 2–3 mg of protein was loaded on a single slab gel. After electrophoresis, the stained H1 bands were cut off from gels and processed according to the procedure of Wu et al. (1982). *Physarum* H1 isolated by the above procedure was lyophilized and used for amino acid analysis.

Isolation of Histone H1 from Calf Thymus. The crude preparation of histone H1 from calf thymus was isolated by the NaCl–citrate method of Johns (1964) and further purified by chromatography on Amberlite CG-50 resin (200–400 mesh) by the method of Kinkade & Cole (1966).

Polyacrylamide Gel Electrophoresis. Protein was routinely analyzed by nondenaturing (acetic acid–urea system) and denaturing ($NaDodSO_4$ system) electrophoreses in 0.15 × 20 × 20 cm polyacrylamide slab gels. Acrylamide gel electrophoresis to resolve phosphorylation levels of H1 was a modification of the method of Panyim & Chalkley (1969). The separating gel contained 14% acrylamide, 0.08% methylenebis(acrylamide), 2.5 M urea, and 5% acetic acid. The 3.5 cm long stacking gel contained 6% acrylamide, 0.08% methylenebis(acrylamide), 2.5 M urea, and 5% acetic acid. The electrophoresis buffer was 0.9 M acetic acid. After preelectrophoresis at 350 V overnight, gels were loaded with 1 M cysteamine and run 2 h at 220 V to scavenge free radicals (Alfageme et al., 1974). After scavenging, the wells were washed, and samples (5–10 μg of protein/well) were loaded in the sample buffer containing 0.9 M acetic acid, 2% β-mercaptoethanol, 2.5 M urea, and 0.01% Pyronine Y tracking dye. Electrophoresis was carried out at 110–120 V until the dye reached the separating gel and then for 24 h at 220 V. Electrophoresis was at room temperature with the main buffer tank cooled with circulating tap water. After electrophoresis, gels were stained for 2 h with Coomassie blue dissolved in methanol–water–acetic acid (5:5:1) and destained by diffusion in hot 7% acetic acid. $NaDodSO_4$–polyacrylamide gel electrophoresis was performed according to Laemmli (1970) except that the separating gel (15% acrylamide) contained a linear gradient (0.4–0.8%) of methylenebis(acrylamide). Electrophoresis was for 20–24 h at 200 V at room temperature. After electrophoresis, gels were soaked in 50% (w/v) Cl_3CCOOH for 1 h and stained and destained as described for acetic acid–urea gels. For the autoradiography, gels were dried on

Whatman 3MM paper in a vacuum chamber, covered with Kodak X-ray films, and exposed. For the fluorography, gels were processed according to the procedure of Bonner & Laskey (1974), dried as for the autoradiography, and exposed to Kodak X-ray films.

Digestion of H1 with Chymotrypsin. The digestion of *Physarum* H1 with chymotrypsin was according to Mende et al. (1983) except that the reaction was terminated by the addition of an equal volume of 2 times concentrated sample buffer for $NaDodSO_4$ gel electrophoresis and boiling for 5 min.

Digestion of H1 with Alkaline Phosphatase. Physarum histone H1 was dissolved at 100–250 μg/mL in a solution containing 0.1 mM $ZnCl_2$ and 60 mM tris(hydroxymethyl)-aminomethane hydrochloride (Tris-HCl), pH 8.0, to which 2 units/mL alkaline phosphatase from *Escherichia coli* (P-L Biochemicals) was added. The reaction was carried out at 37 °C and terminated as described for the digestion with chymotrypsin.

Amino Acid Analysis. A total of 0.5–1 mg of lyophilized *Physarum* H1 isolated by preparative $NaDodSO_4$ gel electrophoresis and electroelution was hydrolyzed for 24 h at 105 °C in 6 M HCl (Merck, Suprapur) containing 0.02% β-mercaptoethanol, in vacuo. After hydrolysis, samples were dried over solid NaOH, dissolved in a buffer, and run on a Beckman amino acid analyzer. Values were not corrected for hydrolytic losses and cysteine was not separately determined.

RESULTS

Source of Electrophoretic Heterogeneity of Physarum H1. Physarum histone H1 isolated by the guanidine hydrochloride method either from nuclei or from solubilized chromatin gives a heterogeneous band when analyzed by $NaDodSO_4$–polyacrylamide gel electrophoresis (Figure 1, upper panel, lanes A and A′). The bulk of this heterogeneity comes from the modification of H1 by phosphorylation. Figure 1 (upper panel) shows the electrophoretic analysis in the $NaDodSO_4$ gel of the dephosphorylation reaction carried out in vitro by the alkaline phosphatase from *E. coli* added to histone H1 isolated from log-phase microplasmodia grown continuously in [^{32}P]orthophosphate. When the pattern of stained proteins (Figure 1, upper panel) is compared to the corresponding autoradiogram (Figure 1, middle panel), it can be seen that phosphates are removed from H1 molecules in the course of the reaction. With the progressing dephosphorylation, the H1 attains a stable, narrow-band appearance on the gel. Its position remains stable also after very long digestion times (Figure 1, lower panel). The partial disappearance of H1 after long incubation seen particularly in lanes H and I is probably due to contamination of phosphatase by some proteolytic activity. The results of Figure 1 show that phosphorylated *Physarum* H1 has lower electrophoretic mobility on $NaDodSO_4$ gels than the nonphosphorylated H1. However the band corresponding to the end product of the dephosphorylation reaction has still the markedly lower mobility on the gel than the fastest migrating band (marked L) of the heterogeneous H1 (Figure 1, compare for example lanes F and A′ in the upper panel, see also the double appearance of H1 band after very long digestion with phosphatase in lanes G and H of the lower panel). The precise superposition of the stained gel and its autoradiogram on Figure 1 reveals that the L band bears no radioactive phosphate. The reason for the persistence of two bands after prolonged phosphatase treatment could be that either the phosphatase did not remove a certain amount of phosphates from H1 or the H1 band was composed of two different sequence variants of which the smaller was not phosphorylated. The third possibility was that both the end product of the dephosphorylation and the L band were the same H1 differing in some other postsynthetic modifications.

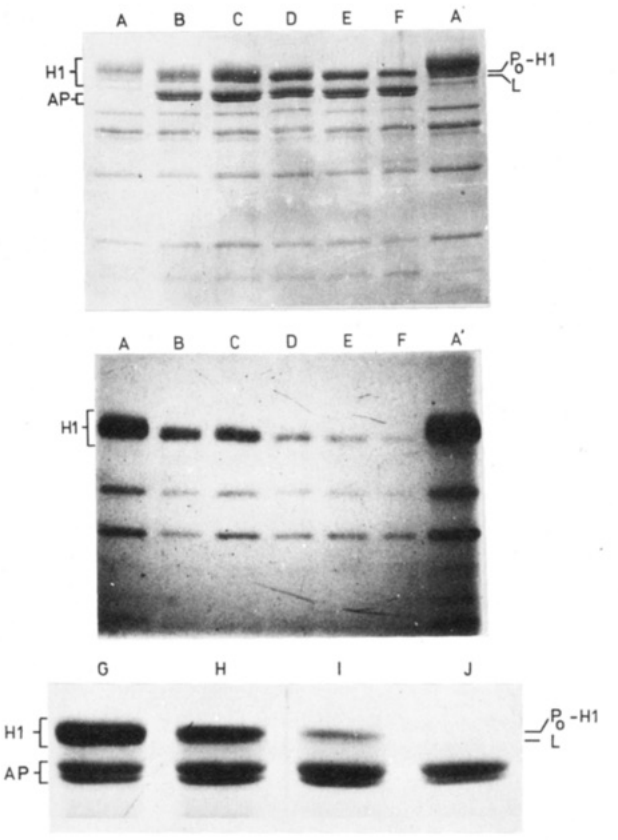

FIGURE 1: Effect of alkaline phosphatase on mobility of *Physarum* H1 in $NaDodSO_4$–polyacrylamide gels. H1 was prepared from log-phase microplasmodia grown continuously in the presence of $^{32}PO_4$ (upper panel) or in nonradioactive medium (lower panel) and dissolved at 0.2 mg/mL. To this, $ZnCl_2$ and Tris-HCl, pH 8.0, were added to final concentration of 0.1 and 60 mM, respectively. After saving one-fifth of the reaction mixture for controls, the rest was preincubated for 3 min at 37 °C, and the reaction was started by addition of 1 unit of alkaline phosphatase from *E. coli*. Radioactive samples of one-tenth of the volume of the reaction mixture were taken during incubation and analyzed on $NaDodSO_4$–polyacrylamide gel electrophoresis (upper panel) and autoradiographed (middle panel). (A) Control (not incubated) without phosphatase; (A′) control incubated at 37 °C for 60 min without phosphatase; (B) 1, (C) 3, (D) 10, (E) 20, and (F) 60 min of incubation at 37 °C with phosphatase. From the digest of nonradioactive H1 (lower panel), samples were taken after (G) 1, (H) 4, and (I) 8 h of incubation at 37 °C with phosphatase and analyzed by $NaDodSO_4$–polyacrylamide gel electrophoresis. (J) Alkaline phosphatase alone. (AP) Position of alkaline phosphatase; (L) position of the fastest migrating band in heterogeneous *Physarum* H1.

The analysis of *Physarum* H1 by ion exchange chromatography on Amberlite CG-50 eluted with linear gradient of guanidine hydrochloride did not show the existence of distinct subspecies that were easily resolved for calf thymus H1 under similar conditions (results not shown). However, this could not rule out the existence of a smaller sequence heterogeneity in *Physarum* H1 not detectable under the gradient conditions employed.

High-Resolution Acetic Acid–Urea Gel Electrophoresis of Physarum H1 from Log-Phase Microplasmodia. The amount of phosphate groups in *Physarum* H1 was estimated by high-resolution acetic acid–urea gel electrophoresis according to Panyim & Chalkley (1969). This method is capable of resolving H1 molecules differing by only one phosphate group (Panyim & Chalkley, 1969; Ajiro et al., 1981). Figure 2 shows the electrophoretic analysis of the products of digestion with alkaline phosphatase of H1 isolated from log-phase micro-

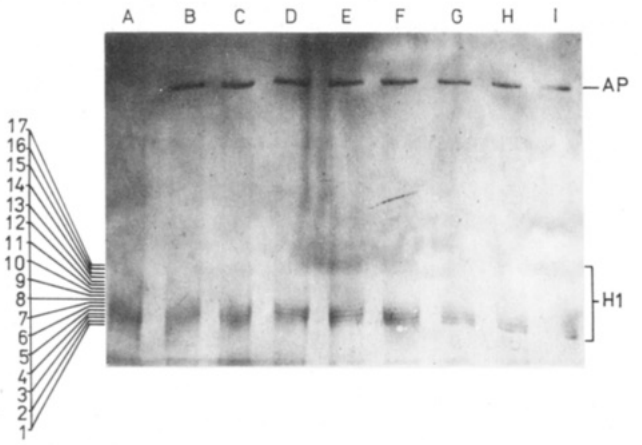

FIGURE 2: Effect of alkaline phosphatase on mobility of *Physarum* H1 in high-resolution acetic acid–urea polyacrylamide gel electrophoresis. H1 from log-phase microplasmodia was digested with alkaline phosphatase as described in Figure 1. Samples from the digestion mixture were analyzed by the high-resolution acetic acid–urea polyacrylamide gel electrophoresis described under Materials and Methods. (A) Control (not incubated); (B) 1, (C) 3, (D) 5, (E) 10, (F) 20, (G) 40, (H) 90, and (I) 120 min of incubation at 37 °C with alkaline phosphatase. (AP) Position of alkaline phosphatase.

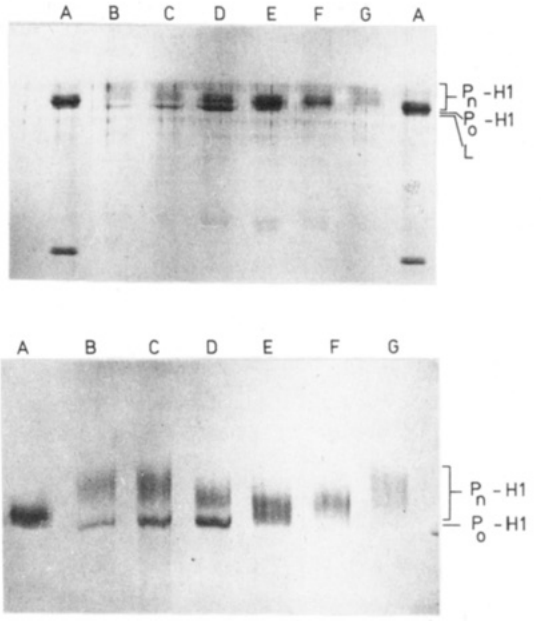

FIGURE 3: Mitotic cycle changes in *Physarum* H1 mobility in Na-DodSO$_4$–polyacrylamide and acetic acid–urea–polyacrylamide gels. Histone H1 was prepared from whole, synchronously grown macroplasmodia taken at different stages of a 8.5-h mitotic cycle, between mitosis II and III. Material was collected by scraping macroplasmodia from the filter paper and immediate freezing at –35 °C. Two to three macroplasmodia were taken for each point in mitotic cycle. The isolated H1 was analyzed by NaDodSO$_4$ (upper panel) and acetic acid–urea (lower panel) gel electrophoresis. (A) Standard preparation of H1 from log-phase microplasmodia; (B) metaphase/anaphase; (C) early S phase; (D) late S phase; (E) middle G2 phase; (F) late G2 phase; (G) early prophase. (P_0-H1) Position of the end product of dephosphorylation in standard microplasmodial H1; (P_n-H1) position of phosphorylated H1; (L) position of the fastest migrating band in the heterogeneous H1.

plasmodia. In the undigested H1 one can count on a stained gel at least 17 evenly spaced bands each representing an integral number of phosphates per H1 molecule (Figure 2, lane A; the contrast of the photograph in Figure 2 does not match that of the original gel). The maximum number of separate bands in undigested, microplasmodial H1 is probably even higher than that since there is some more very faint bands in the upper part of the pattern seen on the original gel. It can be seen that there is a linear dependence between the number of phosphates per H1 molecule and the decrease in the mobility of H1 in the acetic acid–urea gel electrophoresis system. The number of bands decreases gradually in the course of the digestion with phosphatase (Figure 2, lanes B–I), which is most clearly seen for longer digestion times (lanes G–I). The position of the accumulating, lowest band on lane I roughly coincides with that of the fastest migrating band in control sample (land A). It could thus represent the end product of the dephosphorylation. Some discrepances between the number of phosphates on Figure 2 and the amount of radioactivity on the autoradiogram in Figure 1 for comparable times of digestion could be due to a different ratio of H1 to phosphatase in the two experiments. From results of Figure 2, it can be concluded that histone H1 from the log-phase microplasmodia occurs in molecular forms containing from 0 to 17 (and probably more) phosphates. The bulk of it contains between five and nine phosphates per molecule.

Pattern of Phosphorylation of H1 in Mitotic Cycle. To determine the phosphorylation pattern of histone H1 in the mitotic cycle, we isolated it from the synchronously grown macroplasmodia at different stages between mitosis II and III and analyzed it in denaturing and nondenaturing gel electrophoresis systems (Figure 3). The patterns of phosphorylation seen in both systems resemble very closely the pattern observed for *Physarum* H1 by Fischer & Laemmli (1980). In metaphase/anaphase (lane B), early S phase (lane C), and late S phase (land D), a band occurs which in NaDodSO$_4$ gel has the mobility of the L band of the heterogeneous microplasmodial H1. (Note that *Physarum* lacks G1 phase and the synthesis of DNA starts immediately after the metaphase.) This nonphosphorylated band has been shown by Fischer & Laemmli (1980) to be the newly synthesized H1 in contrast to more slowly migrating, phosphate-containing old H1. Indeed it is this band that disappears from the H1 pattern when the protein synthesis is blocked with cycloheximide (see Figure 6). In macroplasmodia with 8.5-h cycle, the observed period of accumulation of the newly synthesized H1 (between 0 and 90 min after metaphase) well correlates with the period of DNA synthesis (Holt, 1980).

From the middle G2 phase (lane E) occurs a gradual phosphorylation of the newly synthesized H1, which is reflected by a decrease in its electrophoretic mobility. The maximum level of phosphorylation is reached in early prophase (lane G) at about 30–40 min before metaphase and is maintained throughout the whole mitosis (lane B) and until the early S phase (20–30 min after metaphase) of the next cycle (lane C).

The resolution of the acetic acid–urea gel electrophoresis used for the analysis of H1 in the mitotic cycle was lower than that in Figure 2. However, due to a linear dependence between the number of phosphates and the decrease of the mobility of histone H1 in acetic acid–urea gels, the comparison of the data of Figure 2 with the relative mobilities of microplasmodial (lane A) and mitotic (lane B) H1 on acetic acid–urea gel in Figure 3 enables the rough estimate of the amount of phosphates per H1 molecule. Thus, assuming seven phosphates to be the average level of phosphorylation of the bulk of microplasmodial H1, the mitotic H1 (lane B) would have from 14 to 28 phosphates per molecule and H1 in the late S phase (lane D) from 8 to 20 phosphates per molecule. The minimum level reached in the middle G2 phase would be from 6 to 14 phosphates per molecule. Although the apparent degree of phosphorylation might not be accurate in an absolute sense, the above calculations do allow a comparison of relative extents of phosphorylation throughout the mitotic cycle.

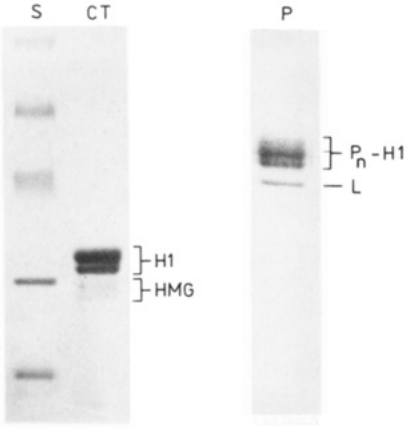

FIGURE 4: Calf thymus H1 and *Physarum* mitotic H1 in NaDod-SO_4–polyacrylamide gel electrophoresis. Calf thymus H1 was isolated by the method of Johns (1964). *Physarum* histone H1 was isolated from five synchronous macroplasmodia taken at metaphase/anaphase of mitosis IV, as described in Figure 3. (S) Molecular weight standards; (CT) calf thymus; (P) *Physarum*; (L) position of the fastest migrating band in heterogeneous *Physarum* H1; (P_n-H1) position of highly phosphorylated forms of *Physarum* H1.

The data of Figure 3 show that the maximum level of phosphorylation of H1 reached by prophase maintains throughout the whole period of mitosis and decreases only after the DNA synthesis has started, in the early S phase. It is also evident that the once phosphorylated H1 molecules are not dephosphorylated totally in the G2 phase of the next generation but remain at the moderate phosphorylation level of 6–14 phosphates per molecule. Therefore, it is only the mitotic superphosphorylation of H1 that is a cyclic event.

It can be seen from the acetic acid–urea gel electrophoresis on Figure 3 that H1 molecules at every point of the mitotic cycle represent a rather broad population of differently phosphorylated species. On the other hand, on the $NaDodSO_4$ gel the phosphorylated H1 is distributed between a limited number (3–4) of distinctly separated bands rather than form a smear (Figure 4, see also the $NaDodSO_4$ gel in Figure 3). The bands seen on $NaDodSO_4$ gels resemble rather the family of sequence variants of mammalian H1 although some intermediate staining between them can also be seen.

Distribution of Phosphates in Physarum H1. In order to study the distribution of phosphates in the H1 molecule, we used the method of chymotrypsin cleavage of *Physarum* H1 as reported by Mende et al. (1983). The limited action of chymotrypsin cleaves *Physarum* histone H1 into two fragments, the larger COOH-terminal and the smaller NH_2-terminal fragment. This is shown in Figure 5 (for example, lanes A and D). It can be seen from the comparison of undigested and chymotrypsin-cleaved H1 that the heterogeneity of the native H1 band is preserved in the COOH-terminal but not in the NH_2-terminal fragment of the molecule. That the COOH-terminal fragment heterogeneity was due to phosphorylation was indicated by the fact that it disappeared when H1 was treated with alkaline phosphatase prior to chymotrypsin cleavage (results not shown). To check the localization with respect to NH_2- and COOH-terminal fragments of the superphosphorylation occurring at mitosis, we isolated H1 from the early G2 phase and from the metaphase/anaphase macroplasmodia, digested it with chymotrypsin, and analyzed the products by $NaDodSO_4$ gel electrophoresis (Figure 5). It can be seen that both the G2 and the mitotic phosphorylation are localized predominantly in the COOH-terminal fragment of H1 molecule. The COOH-terminal fragment has also a characteristic, fast-migrating component that could correspond

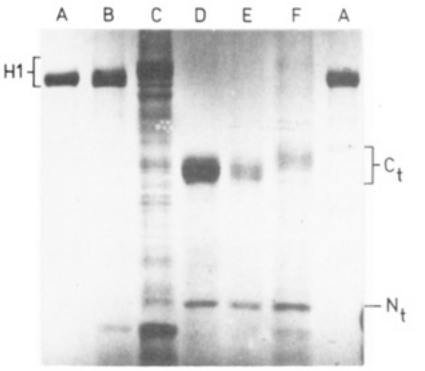

FIGURE 5: Chymotryptic digestion of *Physarum* histone H1 from different stages of the mitotic cycle. Histone H1 was isolated from log-phase microplasmodia and from synchronous macroplasmodia at early G2 and metaphase/anaphase stages of the mitotic cycle as described in Figures 1 and 3, respectively. Part of the isolated H1 was digested with chymotrypsin in 50 mM Tris-HCl, pH 8.0 (enzyme to protein ratio was approximately 1:200), and the samples were analyzed by $NaDodSO_4$ gel electrophoresis. (A) Undigested microplasmodial H1; (B) undigested early G2 H1; (C) undigested metaphase/anaphase H1; (D) chymotrypsin-digested microplasmodial H1; (E) chymotrypsin-digested early G2 H1; (F) chymotrypsin-digested metaphase/anaphase H1; (C_t) COOH-terminal fragment of H1; (N_t) NH_2-terminal fragment of H1.

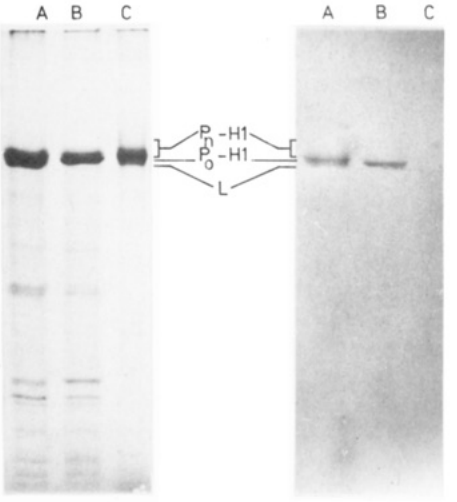

FIGURE 6: $NaDodSO_4$ gel electrophoresis of L-[*methyl*-^{3}H]-methionine-labeled histone H1 from *Physarum*. Histone H1 was isolated from log-phase microplasmodia grown for 8 h in the presence of L-[*methyl*-^{3}H]methionine without (A) and with (B) cycloheximide (10 μg/mL). Conditions of labeling were as described under Materials and Methods. (C) H1 from log-phase microplasmodia grown in nonradioactive medium. (Left panel) Coomassie blue stained gel; (right panel) corresponding fluorogram (exposure was 9 days). (P_n-H1) Position of phosphorylated H1; (P_0-H1) position of the end product of dephosphorylation; (L) position of the fastest migrating band of heterogeneous H1.

to the L band of the intact molecule. The COOH-terminal fragment seems to be a main acceptor of postsynthetic modifications in *Physarum* H1. It should be however stressed that the results of Figure 5 do not rule out the presence of minor modifications in the NH_2-terminal region of H1, not affecting the mobility in $NaDodSO_4$ gels.

Origin of the Fast Migrating L Band. We further assumed that the fastest migrating L band and the end product of dephosphorylation could differ in some postsynthetic modifications other than phosphorylation. A much better resolution of the L band on denaturing $NaDodSO_4$ gels than on acetic acid–urea gels suggested the nonpolar type of modifications out of which the methylation was a prime candidate. Figure 6 shows the stained electrophorogram of the $NaDodSO_4$ gel

Table I: Amino Acid Composition (mol %) of *Physarum* Histone H1

	this work[a]	Mende et al. (1983)	Fisher & Laemmli (1980)
Lys	26.0	17.6	19.3
His	2.3	3.8	0.6
Arg	7.1	5.2	1.7
Asx	3.6	4.0	4.8
Thr	4.7	6.7	6.8
Ser	8.2	8.7	11.3
Glx	9.2	6.8	7.9
Pro	10.3	10.2	12.0
Gly	4.0	4.6	6.6
Ala	17.2	18.1	20.4
Cys	nd	0.2	0.0
Val	2.1	3.7	2.2
Met	0.2	0.8	0.0
Ile	0.8	2.8	2.0
Leu	2.1	3.7	3.0
Tyr	1.0	1.6	0.7
Phe	1.2	1.6	0.7

[a] Data obtained in this work for H1 isolated as described under Materials and Methods and purified by preparative $NaDodSO_4$ gel electrophoresis.

and the corresponding fluorogram of H1 isolated from two log-phase cultures grown for the last 8 h in the presence of [^{3}H]methionine labeled in the methyl group. During the labeling period, the normal growth medium was exchanged for the medium without protein hydrolysate. To one culture, together with the isotope, cycloheximide was added in a concentration known to block completely the protein synthesis in *Physarum* (Bernhardt-Smigielska & Toczko, 1980). It can be seen from the fluorogram that in both isolates (lanes A and B) the label from the [^{3}H]methyl group of methionine was found mainly in H1 bands. The labeling was little affected by the presence of cycloheximide, which rules out the possibility that the label could have been due to incorporation of methionine. In the culture grown without cycloheximide (lane A), the radioactivity is accumulated in a zone including (and extending slightly upward) the position of the end product of the dephosphorylation. The superposition of electrophorogram and fluorogram shows that there is no label in the position of the L band. The stained pattern shows also that the L band is absent in H1 from the cycloheximide-treated culture (lane B). Thus, the L band is the newly synthesized H1. This is consistent with the pattern observed in the mitotic cycle (Figure 3), where the L band appears and accumulates in the S phase.

It can be concluded from the data of Figure 6 that the newly synthezised H1 (the fast-migrating L band) is not methylated in contrast to other H1 classes seen on $NaDodSO_4$ gel. Methylation of the old H1 should therefore be the reason for the difference in the mobility between the L band and the end product of dephosphorylation. Since dephosphorylation by the alkaline phosphatase affects only the intensity of the band corresponding to the end product of dephosphorylation (compare for example the results on Figure 1), the immediate conclusion is that all the phosphorylated H1 molecules are already methylated in an irreversible manner. Thus, already phosphorylated H1 can not undergo methylation. This is consistent with the observation that in the cycloheximide-treated culture (Figure 6, lane B) the radioactivity is restricted to the position corresponding to zero-phosphate H1.

Acceptor of Methyl Groups in H1. In order to obtain a homogeneous H1, we used the method of Wu et al. (1982). The stained H1 band was cut off from the preparative $NaDodSO_4$ gel and electroeluted into the 1% agarose column from

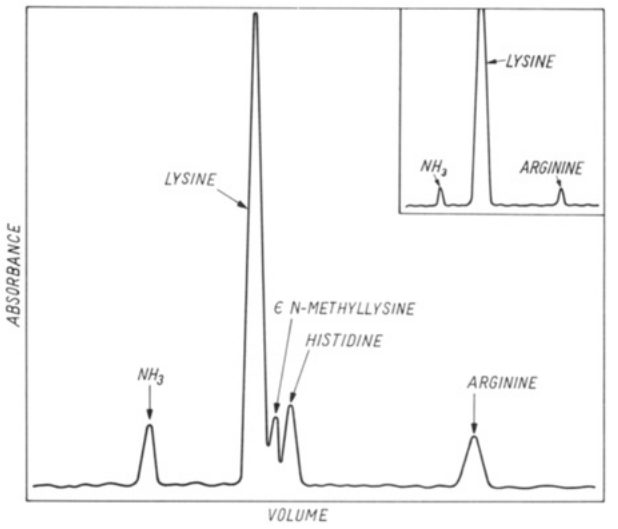

FIGURE 7: Methylation of lysine in *Physarum* histone H1. Fragment of the elution profile obtained with Beckman amino acid analyzer during amino acid analysis of *Physarum* histone H1 purified by electroelution from preparative $NaDodSO_4$ gels as described under Materials and Methods. The abscissa is absorbance after staining with ninhydrin. The peak between lysine and histidine corresponds to the position of N^{ϵ}-methyllysine (Murray, 1964). (Inset) The same fragment of elution profile from amino acid analysis of calf thymus H1 (isolation of calf thymus H1 as described under Materials and Methods; preparation for amino acid analysis as described for Physarum H1). Note the lack of peaks in positions of N^{ϵ}-methyllysine and histidine.

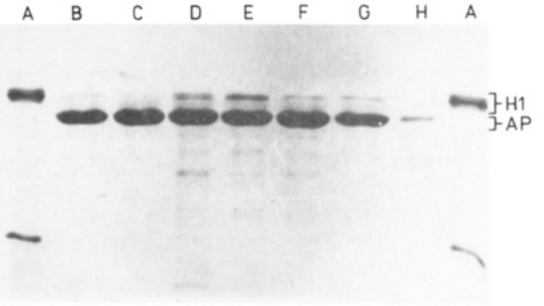

FIGURE 8: Mitotic cycle changes in mobility in $NaDodSO_4$–polyacrylamide gel of *Physarum* H1 dephosphorylated with alkaline phosphatase. Histone H1 was prepared from synchronous macroplasmodia as described in Figure 3. The isolated H1 was dephosphorylated by 60-min incubation at 37 °C with alkaline phosphatase from *E. coli* as described in Figure 1 and analyzed by $NaDodSO_4$ gel electrophoresis. (A) Microplasmodial H1 not treated with alkaline phosphatase; (B) metaphase/anaphase; (C) early S phase; (D) late S phase; (E) middle G2 phase; (F) late G2 phase; (G) early prophase; (H) alkaline phosphatase alone; (AP) position of alkaline phosphatase. In (B) and (C), somewhat less material was loaded.

which it was almost quantitatively recovered. This procedure eliminated the several contaminations of H1 seen in Figure 1. The amino acid composition of the protein recovered from the agarose gel is typical for H1 (Table I) and resembles closely the composition reported for *Physarum* H1 by others (Fischer & Laemmli, 1980; Mende et al., 1983). The amino acid analysis has also revealed the existence of a single peak eluting immediately after lysine and before histidine and at identical position as that reported by Murray (1964) for N^{ϵ}-methyllysine (Figure 7). We did not attempt to distinguish between mono- and dimethyllysine to precisely evaluate the amount of N^{ϵ}-methyllysine. As it can be seen from Figure 7, the majority of lysines in *Physarum* H1 occur in non-methylated form.

Pattern of Methylation of H1 in Mitotic Cycle. Figure 8 shows the $NaDodSO_4$ gel electrophoresis of alkaline phos-

phatase treated H1 isolated from the synchronously grown macroplasmodia taken at the same points in the mitotic cycle as those in Figure 3. It seems to be a precursor–product like relationship between the nonmethylated H1 (the fast-migrating L band) and the zero-phosphate band (the end product of dephosphorylation) of H1. The nonmethylated H1 seen at the highest concentration at the time of maximum DNA synthesis (lane D) is gradually moving upward on the gel, through the intermediate stages, to reach the position of the zero-phosphate band by the second half of the G2 phase (lane F).

From the data of Figures 3 and 8, it can be concluded that the newly synthesized histone H1 is deposited on DNA during the S phase in the nonmethylated form. The irreversible methylation of ϵ-NH_2 groups of several of its lysines starts at the end or even after the S phase and continues until, by the second half of the G2 phase, 100% of the new H1 is totally methylated.

Discussion

Phosphorylation of H1. The pattern of phosphorylation of *Physarum* H1 during the mitotic cycle has been a matter of concern over the past few years. Bradbury et al. (1974) reported a peak in H1 phosphorylation occurring shortly before metaphase. Later, Fischer & Laemmli (1980) using a radioisotope labeling that allowed them to identify the newly synthesized and the old H1 on $NaDodSO_4$ gels confirmed the increase in the H1 phosphate content in prophase but failed to find any significant dephosphorylation of H1 either during or shortly after mitosis. By following the fate of radio phosphate incorporated into H1 in late G2 phase by two succesive mitosis, they also showed that during this prolonged chase there was only a gradual loss of radio phosphate at about 50% per generation. Fischer and Laemmli concluded from their studies that since there was no significant dephosphorylation following metaphase, the dephosphorylation of H1 can not be a prerequisite for chromosome condensation.

In this study, we used two electrophoretic systems, the denaturing $NaDodSO_4$ system and the nondenaturing acetic acid–urea system, to analyze the fate of the total, unlabeled H1 during the mitotic cycle. With the $NaDodSO_4$ system, we obtained virtually the same results as Fischer & Laemmli (1980) so we assumed that there was no need to repeat their radioisotope pulse–chase studies. However, the real picture of the phosphorylation of this same H1 could only be seen on the nondenaturing acetic acid–urea gel, which is sensitive to charge rather than conformational differences. Analyzing the fate of H1 by the acetic acid–urea gel electrophoresis and correlating it with the data from $NaDodSO_4$ gel electrophoresis (Figure 3, upper and lower panel) and the radioisotope chase experiment of Fischer & Laemmli (1980), we found the following pattern of the phosphorylation of H1 during the 8.5-h mitotic cycle. After the S phase (about 1.5 h after metaphase) the newly synthesized H1 becomes gradually phosphorylated accepting from 8 to 16 phosphates per molecule by the second half of the G2 phase (about 6.5 h after metaphase). Between the late G2 phase and prophase, all H1 molecules undergo mitotic superphosphorylation, accepting from 14 to 28 phosphates per molecule. The upper limit of the number of phosphates may not be very accurate here; it is however worth noting that the unusually high number of phosphorylated sites in *Physarum* H1 has been also reported recently by Yasuda et al. (1984). H1 remains in the superphosphorylated state throughout the whole mitosis until the begining of DNA synthesis in the next S phase. From the early S phase (about 0.5 h after metaphase) a gradual dephosphorylation occurs that however, removes only a part of phosphates from H1. It has still from about 8 to about 16 phosphates per molecule in the middle G2 phase and about that number of phosphates preserves up to the begining of the next mitotic superphosphorylation.

The above pattern is strictly consistent with the 50% loss of chased radio phosphate per generation reported by Fischer & Laemmli (1980). Due to the features of the $NaDodSO_4$ gel electrophoresis, Fischer & Laemmli could not precisely distinguish between the relatively high phosphate content in the G2 phase and the superphosphorylation of H1 in mitosis. The most important conclusions from the above picture are the following: (1) The phenomenon of cyclic, mitotic superphosphorylation of H1 characteristic of the replicating mammalian cells occurs also in the lower eukaryote *Physarum*. It is however superimposed on the unusually high level of the interphase phosphorylation of H1. (2) The phosphorylation of newly deposited H1 starts well after the end of S phase.

Correlation between Methylation and Phosphorylation of H1. This work shows for the first time that histone H1 can be modified in chromatin by the methylation of the ϵ-NH_2 groups of lysines. The data obtained are consistent with the interpretation that the newly synthesized H1 is deposited onto DNA in the nonmethylated form. This is supported by the position of the new H1 on $NaDodSO_4$ gels in mitotic cycle studies (Figure 3), the pattern of H1 methylation in the mitotic cycle (Figure 8), and the experiments with labeling H1 with L-[*methyl*-^{3}H]methionine (Figure 6). On the other hand, the lack of accumulation of the nonmethylated H1 during in vitro dephosphorylation of isolated *Physarum* H1 with alkaline phosphatase (Figure 1) as well as the lack of label from [^{3}H]methionine in already phosphorylated forms of H1 in cycloheximide-treated culture (Figure 6) is consistent with the assumption that the phosphorylation of H1 is preceded by its methylation. This is in agreement with the timing of methylation of the new H1 in the mitotic cycle (Figure 8). Similarly to phosphorylation, it occurs rather late in the cycle, between the end of S phase and a point somewhere in between the middle and the late G2 phase. The schematic interpretation of the data concerning the methylation and the phosphorylation of H1 during the mitotic cycle is shown in Figure 9.

The mitotic cycle analysis indicates that methylation is irreversible and concerns all H1 molecules associated with DNA. In contrast to phosphorylation which yields at every point in the mitotic cycle a population of differently phosphorylated H1 molecules, methylation seems to modify uniformly all the molecules of H1 at least as far as the mobility in $NaDodSO_4$ gel electrophoresis is concerned.

We have shown that the phosphorylation of multiple sites in *Physarum* H1 results in the formation of discrete classes as revealed by high-resolution $NaDodSO_4$ gel electrophoresis (Figure 3, upper panel, and Figure 4). Since the $NaDodSO_4$ gel electrophoresis does not separate proteins on the charge basis, it can be argued that these are the true conformational variants of H1. A relatively small number of conformational variants in comparison to the number of phosphorylated sites could mean that multiple phosphorylations are needed to bring about a unit conformational transition in *Physarum* H1. It is interesting that different conformational variants of *Physarum* H1 coexist in chromatin at every stage of the mitotic cycle. It is perhaps worth noting that conformational variants of *Physarum* H1 show no less a difference in mobilities on $NaDodSO_4$ gel electrophoresis than the true sequence variants of calf thymus H1 (Figure 4). Whether different sequence variants of mammalian H1 and multiple conformational classes

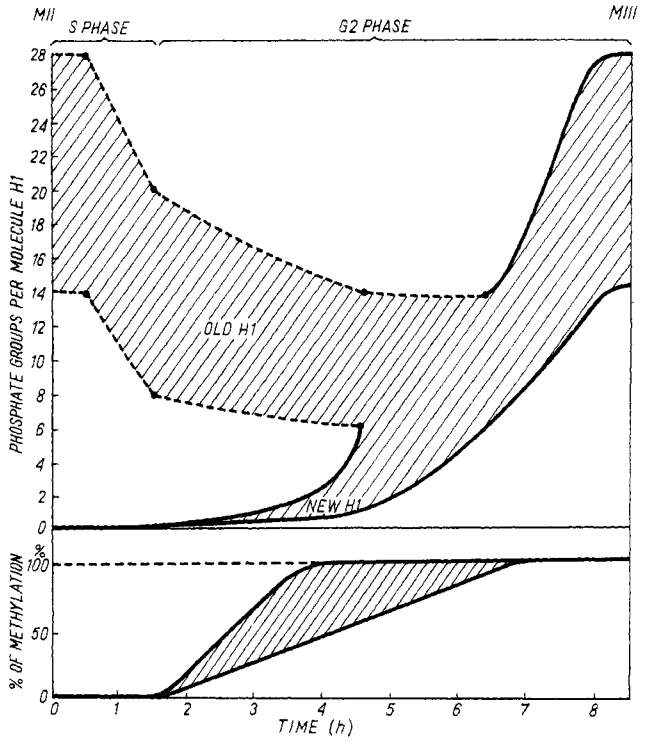

FIGURE 9: Diagrammatic representation of postsynthetic modifications of histone H1 in the mitotic cycle of *Physarum*. Hatched area represents the population of H1 molecules bearing different amounts of modifing groups. Dotted lines represent old and solid lines newly deposited H1. The upper level of phosphorylation may not be accurate.

of the less sequentially heterogeneous *Physarum* H1 reflect two different evolutionary mechanisms aimed to reach the same goal can be of course only a matter of speculation.

The unique postsynthetic methylation of H1 occurring in *Physarum* allows a clear distinction between the fate of old and new H1 in the mitotic cycle. The results of this work indicate that as far as postsynthetic modifications are concerned the old and the new H1 progress through the mitotic cycle via separate routes until the late G2 phase. It is only the massive mitotic superphosphorylation of already fully methylated H1 that seems to affect identically old and new H1.

Distribution of Modifications in Histone H1. It has been demonstrated that in *Physarum* H1 the phosphorylations (including the mitotic superphosphorylation) are mainly found in the large COOH-terminal fragment of the molecule (Figure 5). The same could be true for methylation although this needs further studies with isotope labeling. These facts point to the importance of the proper conformation of the COOH-terminal fragment of H1 for its function in chromatin. It remains to be answered whether the high level of interphase phosphorylation as well as the methylation of *Physarum* H1 does to some extent compensate for its abnormally high molecular weight (Mende et al., 1983). It should be noted that the repeat length of *Physarum* chromatin is not much different from that of mammalian chromatin (Johnson et al., 1976; Staron et al., 1977). Still to be elucidated is the link between the mitotic superphosphorylation of H1 and chromatin condensation in mitosis.

In the light of this work, *Physarum* offers considerable advantages in studying several of the above-mentioned problems. The sequence variability of *Physarum* H1, if existent, is by far less pronounced than in mammalian systems, which makes the studying of the role of postsynthetic modifications much easier. The unusually high level of phosphorylation in *Physarum* H1 can also facilitate studies on the role of this modifications in H1–DNA and H1–protein interactions.

ACKNOWLEDGMENTS

We thank Professor Aloys Huttermann (Universitat Gottingen) for his help in obtaining some reagents needed for this work. We are grateful to A. Bakuła and A. Szymanński for excellent technical help and to Drs. T. Motyl and W. Kukulska for performing amino acid analysis.

REFERENCES

Ajiro, K., Borun, T. W., & Cohen, L. H. (1981) *Biochemistry 20*, 1445–1454.

Alfageme, C. R., Zweidler, A., Mahowald, A., & Cohen, L. H. (1974) *J. Biol. Chem. 249*, 3729–3736.

Bernhardt-Smigielska, J., & Toczko, K. (1980) *Acta Biochim. Pol. 27*, 221–231.

Bonner, W. M., & Laskey, R. A. (1974) *Eur. J. Biochem. 46*, 83–88.

Bradbury, E. M., Inglis, R. J., & Matthews, H. R. (1974) *Nature (London) 247*, 257–261.

Cole, R. D. (1984) *Anal. Biochem. 136*, 24–30.

Daniel, J. W., & Baldwin, H. H. (1964) *Methods Cell Physiol. 1*, 9–41.

Fischer, S. G., & Laemmli, U. K. (1980) *Biochemistry 19*, 2240–2246.

Gurley, L. R., Tobey, R. A., Walters, R. A., Hildebrandt, C. E., Hohmann, P. G., D'Anna, I. A., Barham, S. S., & Deaven, L. L. (1978) in *Cell Cycle Regulation* (Jeter, J. R., Cameron, I. L., Padilla, G. M., & Zimmermann, A. M., Eds.) pp 37–60, Academic Press, New York.

Hohmann, P. G. (1983) *Mol. Cell. Biochem. 57*, 81–92.

Holt, C. E. (1980) in *Growth and Differentiation in Physarum Polycephalum* (Dove, W. F., & Rusch, H. P., Eds.) Princeton University Press, Princeton, NJ.

Jockusch, B. M., & Walker, I. O. (1974) *Eur. J. Biochem. 48*, 417–425.

Johns, E. W. (1964) *Biochem. J. 92*, 55–59.

Johnson, G. C., Littau, V. C., Allfrey, V. C., Bradbury, E. M., & Matthews, H. R. (1976) *Nucleic Acids Res. 3*, 3313–3329.

Kinkade, J. M., & Cole, R. D. (1966) *J. Biol. Chem. 241*, 5790–5797.

Laemmli, U. K. (1970) *Nature (London) 227*, 680–685.

Mende, L. M., Waterborg, J. H., Mueller, R. D., & Matthews, H. R. (1983) *Biochemistry 22*, 38–51.

Mittermayer, C., Braun, R., & Rusch, H. P. (1965) *Exp. Cell Res. 38*, 33–41.

Mohberg, J. (1975) in *The Cell Nucleus* (Busch, M., Ed.) Academic Press, New York.

Murray, K. (1964) *Biochemistry 3*, 10–14.

Panyim, S., & Chalkley, R. (1969) *Arch. Biochem. Biophys. 130*, 337–346.

Staroń, K., Jerzmanowski, A., Tyniec, B., Urbańska, A., & Toczko, K. (1977) *Biochim. Biophys. Acta 475*, 131–138.

Thoma, F., Koller, T., & Klug, A. (1979) *J. Cell Biol. 83*, 403–427.

Wu, R. S., Stedman, J. D., West, M. H. P., Pantazis, P., & Bonner, W. M. (1982) *Anal. Biochem. 124*, 264–271.

Yasuda, H., Mueller, R., & Bradbury, E. M. (1984) *Abstracts of Papers*, 6th European Physarum Workshop, Font Romeu, France, April 1984, CNRS Touluse.